Resolving the phylogenetic position of Darwin's extinct ground sloth (Mylodon darwinii) using mitogenomic and nuclear exon data

Frédéric Delsuc, Melanie Kuch, Gillian C Gibb, Jonathan Hughes, Paul Szpak, John Southon, Jacob Enk, Ana T Duggan, Hendrik N Poinar

PROCEEDINGS OF
THE ROYAL SOCIETY B
BIOLOGICAL SCIENCES

Resolving the phylogenetic position of Darwin's extinct ground sloth (Mylodon darwinii) using mitogenomic and nuclear exon data

Journal:	*Proceedings B*
Manuscript ID	RSPB-2018-0214.R1
Article Type:	Research
Date Submitted by the Author:	n/a
Complete List of Authors:	Delsuc, Frédéric; Institut des Sciences de l'Evolution, CNRS, IRD, EPHE, Université de Montpellier Kuch, Melanie; McMaster University, Department of Anthropology Gibb, Gillian; Massey University, Ecology Group, Institute of Agriculture and Environment Hughes, Jonathan; McMaster University, Department of Anthropology Szpak, Paul; Trent University, Department of Anthropology Southon, John; University of California, Earth Systems Science Department Enk, Jacob; McMaster University, Anthropology; MYcroarray Duggan, Ana; McMaster University, Department of Anthropology Poinar, Hendrik; McMaster University, 2McMaster Ancient DNA Centre, Departments of Anthropology & Pathology and Molecular Medicine
Subject:	Evolution < BIOLOGY, Genomics < BIOLOGY, Palaeontology < BIOLOGY
Keywords:	Mylodon darwinii, Xenarthra, Ancient DNA, Mitochondrial genomes, Nuclear data, Phylogenetics
Proceedings B category:	Evolution

Resolving the phylogenetic position of Darwin's extinct ground sloth (*Mylodon darwinii*) using mitogenomic and nuclear exon data

Frédéric Delsuc[1,*], Melanie Kuch[2], Gillian C. Gibb[1,3], Jonathan Hughes[2], Paul Szpak[4], John Southon[5], Jacob Enk[2,6], Ana T. Duggan[2] and Hendrik N. Poinar[2,*]

[1]*ISEM, Université de Montpellier, CNRS, IRD, EPHE, Montpellier, France.*

[2]*McMaster Ancient DNA Centre, Department of Anthropology, McMaster University, Hamilton, ON, Canada.*

[3]*Ecology Group, Institute of Agriculture and Environment, Massey University, Palmerston North, New Zealand.*

[4]*Department of Anthropology, Trent University, Peterborough, ON, Canada.*

[5]*Keck Carbon Cycle Accelerator Mass Spectrometer, Earth Systems Science Department, University of California, Irvine, Irvine, CA, USA.*

[6]*MYcroarray, Ann Arbor, MI, USA.*

[*]Authors for correspondence (Frederic.Delsuc@umontpellier.fr; poinarh@mcmaster.ca).

Running head: The phylogenetic position of *Mylodon darwinii*

Abstract

Mylodon darwinii is the extinct giant ground sloth named after Charles Darwin, who first discovered its remains in South America. We have successfully obtained a high-quality mitochondrial genome at 99-fold coverage using an Illumina shotgun sequencing of a 12,880 year-old bone fragment from Mylodon Cave in Chile. Low level of DNA damage showed that this sample was exceptionally well preserved for an ancient sub-fossil, likely the result of the dry and cold conditions prevailing within the cave. Accordingly, taxonomic assessment of our shotgun metagenomic data showed a very high percentage of endogenous DNA with 22% of the assembled metagenomic contigs assigned to Xenarthra. Additionally, we enriched over 15 kilobases of sequence data from seven nuclear exons, using target sequence capture designed against a wide xenarthran dataset. Phylogenetic and dating analyses of the mitogenomic dataset including all extant species of xenarthrans and the assembled nuclear supermatrix unambiguously place *Mylodon darwinii* as the sister-group of modern two-fingered sloths from which it diverged around 22 million years ago. These congruent results from both the mitochondrial and nuclear data support the diphyly of the two modern sloths lineages, implying the convergent evolution of their unique suspensory behaviour as an adaption to arboreality. Our results offer promising perspectives for whole genome sequencing of this emblematic extinct taxon.

Keywords: *Mylodon darwinii*; Xenarthra; Ancient DNA; Mitochondrial genomes; Nuclear data; Phylogenetics.

1. Background

Darwin's extinct ground sloth (*Mylodon darwinii*) was named by Richard Owen in honour of Charles Darwin who discovered its early remains in South America during the Voyage of the Beagle [1]. Like the vast majority of the Pleistocene megafauna, *M. darwinii* went extinct at the Pleistocene/Holocene boundary, approximately 10,000 years ago [2]. Numerous sub-fossils of *M. darwinii* have been found across the South American southern cone [3], including the famous Mylodon Cave (Cueva del Milodón, Ultima Esperanza, Chile). This cave derives its name from the numerous and exquisitely preserved remains of this ground sloth found inside. The constant, cold, and dry conditions of the cave have enabled the exceptional preservation of *M. darwinii* remains in the form of paleofeces, bones, claws, and even large pieces of mummified skin covered with blond fur, riddled with osteoderms [4]. These sub-fossils were the first non-human samples yielding genuine ancient DNA [5]. Short overlapping mitochondrial DNA fragments of 12S and 16S MT-rRNA [5] and MT-CYTB [6] (550-650 base pairs (bp)), have been PCR-amplified, cloned, and sequenced from *M. darwinii* bones, and shorter MT-CYTB sequences of 150 bp have even been recovered from hairs embedded in a paleofecal sample [7].

Advances in sequencing technology that rely predominantly on short DNA fragments have been a boon for the ancient DNA field, greatly facilitating the assembly of whole mitochondrial genomes in particular [8]. Shotgun Illumina sequencing has been successfully applied to a diversity of Pleistocene sub-fossil bones containing enough endogenous DNA to reconstruct complete mitogenomes. These studies have helped elucidate the phylogenetic affinities of extinct taxa such as Columbian and woolly mammoths [9], steppe bison [10], giant lemurs [11], and South American equids [12] and camelids [13]. Shotgun sequencing of paleofeces has also proven useful for reconstructing the phylogenetic position of the extinct cave hyena and

providing insights into its diet [14]. Recently, Slater et al. [15] have reported a partial and composite *M. darwinii* mitogenome reconstructed by mixing reads obtained by DNA target sequence capture from a bone and a paleofeces both sampled at Mylodon Cave. However, apart from endogenous retroviral sequences [15] no phylogenetically informative nuclear DNA has been obtained to date for this extinct taxon.

Previously published mitochondrial data have suggested a close phylogenetic relationship between *Mylodon* and modern two-fingered sloths of the genus *Choloepus* [5,6,15]. Here, we used Illumina shotgun sequencing to obtain a high-quality, ancient mitogenome from *M. darwinii*, significantly improving upon the previously published one [15]. In addition, and importantly, using target sequence capture, we assembled a complementary supermatrix of seven nuclear exons totalling 15 kilobases (kb) for representatives of all xenarthran genera including the extinct *Mylodon* and all modern sloth species. Our refined phylogenetic and dating analyses of congruent mitogenomic and nuclear data encompassing the full diversity of modern xenarthrans corroborated the close relationship of Darwin's ground sloth with two-fingered sloths (*Choloepus*) from which it is estimated to have diverged some 22 million years ago.

2. Methods

(a) Sample, DNA extraction, library preparation, and shotgun sequencing

The *Mylodon* bone sample (MPI SP57) used here stems from the collection of Svante Pääbo's former lab (Max Planck Institute for Evolutionary Anthropology, Leipzig, Germany) and was collected by Andrew Currant (The Natural History Museum, London, UK) in Mylodon Cave (Ultima Esperanza, Chile). Collagen was extracted and purified from a subsample of the specimen at the University of Western Ontario and AMS radiocarbon-dated at the Keck Carbon

Cycle AMS facility of the University of California Irvine (USA) University of California, Irvine [16].

All manipulations took place in the dedicated ancient DNA facilities of the McMaster Ancient DNA Centre of McMaster University. Following subsampling, 300 mg of bone material were reduced to small particle sizes ranging from 1-5 mm using a hammer and chisel. The subsample was then demineralised with 0.5 ml of 0.5 M EDTA pH 8 at room temperature for 24 h with agitation, and the supernatant removed following centrifugation. The pellet was then digested with 0.5 ml of a Tris-HCl-based proteinase K solution with 20 mM Tris-Cl pH 8, 0.5 % sodium lauryl sarcosine (SDS, Fisher Scientific), 1 % polyvinylpyrrolidone (PVP, Fisher scientific), 50 mM dithiothreitol (DTT), 2.5 mM N-phenacyl thiazolium bromide (PTB, Prime Organics), 2.5 mM calcium chloride (CaCl2), and 250 ug/ml proteinase K. Proteinase digestion was performed at room temperature for 24 h, with agitation. Following centrifugation the digestion supernatant was removed and pooled with the demineralization supernatant. We repeated this process three more times for a total of four rounds of demineralization and digestion. Organics were then extracted from the pooled supernatants using phenol:chloroform:isoamyl alcohol (PCI, 25:24:1), and the resulting post centrifugation aqueous solution was extracted with chloroform. We then concentrated the final aqueous phase with 10 kDA Amicon Ultra-4 centrifugal filters (Millipore) at 4,000 x g, with four washes using 0.1 x TE buffer pH 8 to provide a concentrate of 50 ul. This concentrate was purified using the MinElute PCR Purification kit (QIAGEN) with two washes of 700µL Buffer PE and eluted in 50µL Buffer EB and 0.05% Tween-20. An extraction blank, which represents an aliquot of the extraction buffer minus any sample, was carried alongside the *Mylodon* sample during the entire extraction procedure to monitor for possible external contamination during handling.

We used 25 µL of the DNA extract and of the extraction blank in the Illumina® library preparation as described elsewhere [17] replacing all SPRI bead cleanups with MinElute purification to 20 µL Buffer EB. We did not heat-deactivate the Bst polymerase following the fill-in step and instead purified the reaction with MinElute into 20 µL Buffer EB. The libraries were then index amplified using the common P5 and a set of unique P7 indexing primers [17] in 50 ml reactions consisting of 1 PCR buffer II, 2.5 mM MgCl2, 250 mM Deoxynucleotide (dNTP) mix, 200 nM each forward (P5) and reverse (P7) primer, 2.5 U AmpliTaq Gold™ DNA Polymerase (ThermoFisher Science), and 2 ml (100 ng) of template library. Thermal cycling conditions were as follows: initial denaturation at 95°C for 4 min, 12 cycles of 95°C for 30s, 60°C for 30s, 72°C for 30s, and a final extension at 72°C for 10 min. The amplification was performed using a MJ thermocycler (BioRad). The indexed libraries were finally purified with MinElute to 15µL Buffer EB. A qPCR using 16S MT-rRNA sloth-specific primers was performed on both the *Mylodon* and the blank extract libraries, which we have previously shown to be sensitive to ~10 starting copies. The *Mylodon* library had over 10,000 sloth-specific starting copies whereas the blank library did not show any significant sloth-specific amplification, which is not surprising given the strict conditions under which the experiments were conducted. The *Mylodon* library was sequenced at McMaster Genomics Facility as part of an Illumina HiSeq 1500 lane using single-end 72 bp reads.

(b) Target sequence capture and sequencing

Baits for DNA sequence capture were designed using xenarthran sequences obtained in previous studies [18–20] for the following seven targeted nuclear exons: ADORA3 (321 bp), APOB (2420 bp), BCHE (987 bp), BRCA1 (2835 bp), BRCA2 (3983 bp), RAG2 (441 bp), and TTN (4437 bp). For each exon, 80mer baits were generated with a 4x tiling density. This yielded

137 approximately 20 bp probe spacing, or 60 bp probe overlap. Tiling was flexible to ensure even
138 distribution of baits across the loci, as most loci were not perfect multiples of 20. All baits were
139 then BLASTed against the two-fingered sloth (*Choloepus hoffmanni*; NCBI assembly
140 GCA_000164785.2) and nine-banded armadillo (*Dasypus novemcinctus*; NCBI assembly
141 GCA_000208655.2) genome sequences. Baits with more than one hit and a Tm outside the range
142 35–40°C were conservatively excluded. This generated a final set of 4381 baits that were
143 synthetized as a myBaits kit by MYcroarray (Ann Arbor, MI, USA). Twenty-two of the modern
144 xenarthran libraries previously prepared by Gibb et al. [21], were enriched with the designed bait
145 set in order to capture target sequences representing the seven loci of interest for a representative
146 diversity of Xenarthra (electronic supplementary material, table S1). Enrichment for the *Mylodon*
147 library using the same bait set was conducted in a completely separate ancient DNA facility to
148 avoid contamination. For all libraries, we performed two rounds of enrichments using the
149 methodology previously described in Enk et al. [22].

150 In order to re–amplify the captured sequences, a LibQ Master Mix was prepared. This
151 contained 20µl of KAPA SYBR® FAST qPCR Master Mix (2x), 0.60µl Forward Primer 1469
152 (150nM) and 0.60µl Reverse Primer 1470 (150nM) per reaction. The LibQ Mix was added to the
153 18.8µl of captured template and amplified on a CFX. Amplification cycling protocols were as
154 follows: 95°C for 5 minutes; cycle 12 times through 95°C for 30 seconds, 60°C for 45 seconds;
155 finally hold at 60°C for 3 minutes. Following this, the supernatant was removed and saved,
156 yielding the captured library. This was purified using a MinElute PCR Purification Kit (Qiagen)
157 using their standard protocol, yielding a final enriched and purified library suspended in 15µl of
158 Buffer EB.

159 All libraries to be sequenced were pooled together at varying concentrations with the aim

of creating a single solution containing approximately 250 pM of DNA post size selection. In general, each library was calculated to ideally produce one million reads for sequencing. Libraries then underwent size selection to decrease the amount of non–target DNA and increase sequencing efficiency. Size selection was carried out on a 2% gel (50 ml agarose/1x TAE with 2 µl EtBr). Loading dye equivalent to 1/5 of the library volume was added and samples were then run through the gel for 30 minutes at 100V. A 50 bp ladder was used for determining DNA position and size, and the area from approximately 50 to 150 bp was excised. The excised gel was then purified using a MinElute Gel Extraction Kit (Qiagen) column eluted into 60 µl of Buffer EB. Final pool concentrations prior to sequencing were verified using a 2100 Bioanalyzer (Agilent). Sequencing of the enrichment set was performed at McMaster Genomics Facility on an Illumina MiSeq instrument using 150 bp paired-end reads.

(c) Mitogenome and nuclear exons assemblies

Shotgun sequenced raw reads obtained from the *Mylodon* library were adapter-trimmed using cutadapt v1.1 [23] with a quality score cut-off of 30. Contigs were created by *de novo* assembly of the cleaned reads using ABySS 1.3.4 [24] with default parameters and a range of increasing kmers. The resulting 480,662 non-redundant contigs were mapped to the *Choloepus didactylus* reference mitogenome (NC_006924) using the 'medium low sensitivity' settings in Geneious R9 [25]. Iterative mapping of the reads using the more stringent 'low sensitivity' settings was subsequently used to fill the gaps in the assembly of the 174 successfully mapped contigs. The consensus sequence was called using 50% read agreement and all reads were remapped on the consensus to estimate the depth of coverage. Repeating the same procedure using *Bradypus variegatus* (NC_028501) instead of *C. didactylus* as a reference resulted in the same 174 contigs being mapped and the exact same *Mylodon* mitogenome being reconstructed. The final *Mylodon*

mitogenome was then annotated by alignment to the *C. didactylus* reference genome.

Raw reads containing imperfect index combinations were discarded. Index and adapter sequences were removed and overlapping pairs merged with leeHom [26], and then mapped to all xenarthran reference exon sequences available with a modified version of BWA [27,28] with a maximum edit distance of 0.01 (-n 0.01), allowing a maximum of two gap openings (-o 2) and with seeding effectively disabled (-l 16569). Mapped reads were additionally filtered to those that were either merged or properly paired [29], had unique 5' and 3' mapping coordinates [30], and then restricted to reads of at least 24 bp with SAMtools [31]. The bam files were then imported into Geneious for careful assessment by eye for enrichment success and selection of the best assembly for each sequence depending on the most successful reference sequence. Consensus sequences were called with a 50% threshold and a minimum coverage of 2x with ambiguous nucleotides called at sites where the two reads disagreed and there was no third read. As expected, nuclear capture success was variable among both taxa and loci with sloths and anteaters being successfully enriched for all loci, whereas armadillos presented some loci for which the coverage was insufficient to confidently call a consensus sequence. The capture experiment nevertheless enabled us to produce a total of 144 newly assembled xenarthran sequences for the seven nuclear exons targeted (electronic supplementary material, table S1).

(d) DNA damage and metagenomic analyses

Analyses of post-mortem C to T and G to A mutations in the 53,550 reads mapping to the reconstructed *Mylodon* mitogenome were conducted using mapDamage 2.0 [32]. For comparisons, four modern xenarthran species from Gibb et al. [21] and the extinct glyptodont *Doedicurus* [33] were also analysed. For metagenomic analyses, MEGAHIT v1.1.1 [34] was used to assemble the *Mylodon* shotgun reads. The resulting 385 contigs of more than 200bp were

then subjected to similarity searches against the GenBank nucleotide database (version of 28 April 2017) using MEGABLAST followed by taxonomic assignation using MEGAN 6 with default LCA parameters [35] and subsequent graphical representation with KRONA [36].

(e) Phylogenetic and dating analyses

For constructing the mitogenomic supermatrix, we chose 31 representative living xenarthran species from the dataset of Gibb et al. [21] plus three afrotherian outgroups (electronic supplementary material, table S1). We then added *M. darwinii* sequences (excluding the variable control region) and aligned each gene with MAFFT [37] within Geneious guided by translation for the protein-coding genes. We removed ambiguously aligned sites on each dataset with Gblocks [38] using default relaxed parameters. The final mitogenomic matrix contained 15,222 sites for 35 taxa representing all living xenarthran species plus the extinct *M. darwinii*.

For assembling the seven nuclear exons supermatrix, the newly obtained *Mylodon* and modern xenarthran sequences were added to available sequences plus the same three afrotherian outgroups (electronic supplementary material, table S1). Each exon was then aligned by translation with MAFFT within Geneious. We removed ambiguously aligned codons on each alignment with Gblocks using relaxed default parameters. The final nuclear exons matrix contained 15,216 sites for 28 taxa encompassing all living xenarthran genera and the extinct *M. darwinii* with an overall percentage of missing data of only 16%. Importantly, *Mylodon* was represented at 10,238 unambiguous sites (67.28% of the total) of the nuclear concatenated data set.

The best-fitting partition schemes were determined for both datasets using PartitionFinder v1.1.1 [39]. For the mitogenomic dataset, we used the greedy algorithm on 42 a priori partitions corresponding to codon positions, 12S MT-rRNA, 16S MT-rRNA, and all tRNAs, with unlinked

branch lengths, and using the Bayesian Information Criterion (BIC) for model selection (electronic supplementary material, table S2). For the nuclear dataset, we used the greedy algorithm on 21 a priori partitions corresponding to codon positions, with linked branch lengths, and the BIC for model selection (electronic supplementary material, table S3). For both datasets, ML partitioned reconstruction was conducted with RAxML 8.2.8 [40] using the best-fitting scheme with parameters unlinked across partitions. Maximum Likelihood bootstrap values (BP_{PART}) were obtained after 100 replicates. Bayesian phylogenetic inference under a mixed model was performed using the MrBayes 3.2.3 [41] using the best-fitting scheme with parameters unlinked across partitions. Two independent sets of four MCMCMCs were run for 1,000,000 generations sampling every 1000 generations. After a burn-in of 25%, the 50% majority-rule consensus tree and associated clade posterior probabilities (PP_{PART}) were computed from the 1,500 trees combined in the two independent runs. Bayesian phylogenetic reconstruction was also conducted under the CAT-GTR+G_4 mixture model using PhyloBayes MPI 1.7b [42]. Two independent MCMCs were run for 50,000 cycles sampling every 10 cycles during 2,750,000 tree generations. After a burn-in of 10%, the 50% majority-rule consensus tree and associated clade posterior probabilities (PP_{CAT}) were computed from the 9000 combined trees of the two runs using bpcomp.

Molecular dating analyses were conducted on both datasets using PhyloBayes 3.3f [43] under the CAT-GTR+G_4 mixture model and a log-normal autocorrelated relaxed clock with a birth–death prior on divergence times combined with soft fossil calibrations. We used the same best-fitting relaxed clock model, six fossil calibrations, and priors as in Gibb et al. [21] so that the divergence dates obtained could be directly compared between the two studies. Calculations were conducted in each case by running two independent MCMCs for a total 50,000 cycles

sampling every 10 cycles. The first 500 samples (10%) were excluded as burn-in after convergence diagnostics. Posterior estimates of divergence dates were computed from the remaining 4500 samples of each MCMC using readdiv.

3. Results and Discussion

(a) A new high quality *Mylodon* mitogenome

The radiocarbon date we obtained for the *Mylodon* bone sample MPI SP57 is 12,880 ± 35 ^{14}C yrbp (radiocarbon years before present), which is fully congruent with previous estimates for other samples from Mylodon Cave [2]. Illumina sequencing of the *Mylodon* shotgun library produced a total of 28,020,236 single-end 72 bp reads. Low, yet consistent DNA damage on those reads shows that our ancient *Mylodon* sample was exceptionally well preserved and thus helps support its authenticity (figure 1*a*, electronic supplementary material, figures S1, S2). Estimates of C to T and G to A transitions caused by post-mortem mutations (up to 11% and 8% respectively) were intermediate between those of the subfossil *Doedicurus* sp. osteoderm sample of the same age (up to 25% and 20%) and the *Calyptophractus* museum specimen (up to 4% and 3%), whereas modern xenarthran tissue samples exhibit values below 1%. These values argue in favour of the endogenous origin of the *Mylodon* shotgun reads and set our bone sample among some of the best ancient samples analysed so far [44]. The consistently cold and dry conditions encountered at Mylodon Cave [4] probably explain the exceptional preservation of samples coming from this location [5].

Metagenomic analyses indicate that 30% of the 222 taxonomically assigned contigs (out of a total of 385) are mammalian in origin: 22% are xenarthrans, with 17% matching specifically to the two-fingered sloth (*C. hoffmanni*) genome assembly (figure 1*b*). The only 3% of contigs

assigned to *Homo sapiens* in fact match conserved portions of the mammalian 18S and 45S ribosomal RNA genes and thus could not be considered to represent human specific contamination. Moreover, 25% of the assigned contigs are fungal in origin with *Aspergillus* mold representing 12%. Finally, 35% of the assigned contigs belong to Bacteria, 28% being assigned to the genus *Clostridium* with dominant taxa such as *C. novyi* (13%) and *C. botulinum* (6%) that are commonly found in ancient DNA samples and soil. To further quantify possible contamination from humans or other mammals found in Mylodon Cave such as *Hippidion saldiasi*, *Lama guanicoe*, *Dusicyon avus*, and *Panthera onca mesembrina* [4], we mapped our shotgun reads to available mitogenomes for these species, or to those of closely related ones, using the low sensitivity settings of Geneious. None of the mapping results were convincing apart from a few reads, which mapped to conserved regions of the mammalian mitogenome (data not shown). For instance, we had only 536 reads mapping to conserved regions of the human reference mitogenome (NC_012920), again supporting the authenticity of our sample.

The assembly of 53,550 shotgun reads allowed for the reconstruction of a high quality mitogenome for *M. darwinii* at an average depth of 99x (range 1x-307x). As independent replication is an important component of the ancient DNA research agenda [45], we verified that our consensus sequence matched perfectly to previously obtained PCR fragments attributed to *Mylodon* for the mitochondrial 12S and 16S MT-rRNAs [5] and MT-CYTB [6] genes. However, a comparison with a recently published mitogenome sequence [15] revealed a number of discrepancies (electronic supplementary material, figure S11). The two sequences are identical at only 81% of total sites (89% when excluding ambiguous sites and the control region). The Slater et al. [15] sequence (KR336794) also contains 1383 Ns and presents a substantial number of substitutions in otherwise conserved regions of the sloth mitogenome when compared to *C.*

didactylus, including frameshifting substitutions causing stop codons in 11 out of the 13 coding genes (electronic supplementary material, table S4). These differences most probably represent errors that were spuriously incorporated into the assembly resulting from overall lower coverage depth of the composite mitogenome, reconstructed from captured sequences stemming from both bone and paleofecal material. Mapping the reads produced by Slater et al. [15] (SRA accession SRR2007674) to our *Mylodon* mitogenome confirmed that these divergent regions correspond to regions of low depth of coverage in their capture experiment (data not shown). These errors likely explain an artificially inflated branch length in the phylogenetic tree, potentially impacting the inference of the divergence date between the extinct *Mylodon* and modern sloths (electronic supplementary material, figure S12). Based on these observations, we would recommend using our fully annotated and higher quality mitogenome sequence in future analyses.

(b) Nuclear data corroborate the phylogenetic position of *Mylodon darwinii*

Phylogenetic analyses of our complete xenarthran mitogenomic dataset using Bayesian and ML methods recovered the same strongly supported topology in which *Mylodon* is the sister-group of modern two-fingered sloths of the genus *Choloepus* (figure 2*a*). The statistical support for this phylogenetic position was high with the Bayesian mixture model ($PP_{CAT} = 0.95$) and maximal with the Bayesian and ML partitioned models ($PP_{PART} = 1$; $BP_{PART} = 100$). All other nodes within Pilosa received maximal support from all methods. These results obtained by including the full species diversity of modern sloths add support to the position of *M. darwinii* originally suggested by short mitochondrial PCR fragments [5,6] and recently supported by mitogenomic analyses including fewer taxa [15]. The phylogenetic picture provided by the mitochondrial genome alone could nevertheless be misleading in cases of mito-nuclear discordance caused by factors such as adaptive introgression or past hybridization events [46]. It was thus important to

substantiate our mitogenomic results by nuclear data. In this case, the same phylogenetic analyses applied to the supermatrix of the concatenated seven nuclear exons yield identical results with maximum statistical support placing *Mylodon*, once again as the sister-group of two-fingered sloths (figure 2*b*). Such perfect topological congruence between mitochondrial genomes and nuclear markers provides clear and convincing evidence of the phylogenetic position of the extinct Darwin's ground sloth within the evolutionary history of sloths. These phylogenetic results provide further support for the diphyletic origin of modern sloths implying an independent evolution of arboreality from terrestrial ancestors [47,48] and the independent evolution of their unique suspensory lifestyle resulting in numerous convergent anatomical adaptations [49,50].

Relaxed molecular clock analyses of both the mitogenomic and nuclear datasets recover relatively ancient dates for the common ancestor of sloths (figure 3, table 1). The corresponding divergence between the two modern sloth genera *Bradypus* (Bradypodidae) and *Choloepus* (Megalonychidae) is estimated to be 25 ± 6 Mya with the mitogenomic dataset (figure 3*a*), and 28 ± 4 Mya with the nuclear supermatrix (figure 3*b*). These inferred dates are relatively older than previous estimates based on nuclear data but with reduced taxon sampling [19,51], further justifying their classification into distinct families. The difference with previous nuclear dates might have to do with the CAT-GTR+G4 mixture model which allows for a better correction of substitutional saturation combined with the inclusion of the internal xenarthran calibration points here provided by the earliest fossil cingulate skull [52].

Regarding our extinct sample, our results reveal that *Mylodon* separated from two-fingered sloths of the genus *Choloepus* early in sloth evolutionary history with both datasets clearly agreeing upon a divergence date of about 22 Mya (figure 3, table 1). The dating estimate

obtained with our revised *Mylodon* mitogenome (22 ± 5 Mya; figure 3*a*) is somewhat comparable with previous estimates proposed by Slater et al. [15] based on a different approach. These authors used a recently developed dating method based on the Fossilized Birth-Death (FBD) process that allows one to directly incorporate fossil taxa [53], but requires the use a topological constraint including both fossil and modern taxa. Because of the uncertainty associated with the phylogenetic position of some key sloth fossil taxa, Slater et al. [15] found that their divergence date estimates under the FBD process were highly sensitive to the treatment of ambiguous Deseadan fossil taxa as representing either stem or crown fossil folivorans. By contrast using nodal calibrations and a better sampling of modern species, our results appear intermediate with those obtained with the two alternative treatments. In fact, the diversification of sloth lineages in the Early Miocene (25-22 Mya) corresponds with the end of the first major Bolivian tectonic event, when the Andes became the principal relief of South America, significantly influencing paleoclimates [54]. This period led to a major shift in South American mammalian fossil communities including the Miocene radiation of ground sloths [55]. Our results based on an updated mitogenomic dataset and a new nuclear supermatrix corroborate *M. darwinii* as belonging to a distinct lineage of sloths (family Mylodontidae) originating more than 22 Mya and persisting until their extinction only some 10,000 years BP [56,57].

4. Conclusions and Perspectives

Our study provides a high quality complete mitochondrial genome as well as the first phylogenetically informative nuclear loci for the extinct Darwin's ground sloth. Analyses of these new data, validate the phylogenetic position of *M. darwinii* as a member of a distinct

lineage (Mylodontidae) and as a sister-group to modern two-fingered sloths (genus *Choloepus*; Megalonychidae), originating about 22 million years ago. The exceptional preservation of these cave-preserved *Mylodon* bone samples will enable complete genome sequencing of this emblematic extinct taxon generating further insights into their unique features and ultimate extinction.

Data accessibility. *M. darwinii* mitogenome: GenBank (MF061314). Nuclear exon data: European Nucleotide Archive (LT852562-LT852705). *M. darwinii* shotgun Illumina reads: Sequence Read Archive (ERR1958375). Additional data including bait design, alignments, and trees: Dryad doi:10.5061/dryad.ft3k3.

Competing interests. Jacob Enk is an employee of MYcroarray (Ann Arbor, MI, USA).

Acknowledgments. Andrew Currant and Svante Pääbo kindly provided access to the *Mylodon* bone. We thank the following individuals and institutions for tissue samples: François Catzeflis (Institut des Sciences de l'Evolution, Montpellier, France), Jean-François Mauffrey, Philippe Gaucher, Eric Hansen, François Ouhoud-Renoux, Jean-Christophe Vié, Philippe Cerdan, Michel Blanc, and Rodolphe Paowé (French Guiana), Jorge Omar García and Rodolfo Rearte (Complejo Ecológico Municipal, Presidencia Roque Sáenz Peña, Argentina), Daniel Hernández (Facultad de Ciencias, Universidad de la República, Montevideo, Uruguay), John Trupkiewicz (Philadelphia Zoo, USA), Darrin Lunde (National Museum of Natural History, Washington, USA), Jim Patton and Yuri Leite (Museum of Vertebrate Zoology, Berkeley, USA), Gerhard Haszprunar and Michael Hiermeier (Zoologische Staatssammlung München, Munich, Germany), Géraldine Véron (Museum National d'Histoire Naturelle, Paris, France), Agustín Jiménez-Ruiz,

Nadia Moraes-Barros, and Mariella Superina. We finally thank three anonymous referees for helpful comments. This is contribution ISEM 2018-041-SUD of the Institut des Sciences de l'Evolution de Montpellier.

Authors' contributions. MK, GCG, JH, JE, AD carried out the molecular lab work, participated in data analysis, conducted mitogenome and nuclear data assembly, participated in the design of the study; PS, JS radiocarbon-dated the bone sample; FD carried out DNA damage, metagenomic, sequence alignment, and phylogenetic analyses; FD, HNP conceived of the study, designed the study, coordinated the study, and drafted the manuscript. All authors gave final approval for publication.

Funding statement. FD: Centre National de la Recherche Scientifique (CNRS), the Scientific Council of the Université Montpellier 2 (UM2), and Investissements d'Avenir managed by Agence Nationale de la Recherche (CEBA, ANR-10-LABX-25-01). HNP: Natural Sciences and Engineering Research Council of Canada (NSERC, # RGPIN04184-15) and Canada Research Chairs program.

References

1. Fernicola JC, Vizcaíno SF, De Iuliis G. 2009 The fossil mammals collected by Charles Darwin in South America during his travels on board the HMS Beagle. *Rev. Asoc. Geológica Argent.* **64**, 147–159.

2. Villavicencio NA, Lindsey EL, Martin FM, Borrero LA, Moreno PI, Marshall CR,

414 Barnosky AD. 2016 Combination of humans, climate, and vegetation change triggered Late
415 Quaternary megafauna extinction in the Última Esperanza region, southern Patagonia, Chile.
416 *Ecography* **39**, 125–140. (doi:10.1111/ecog.01606)
417 3. Varela L, Fariña RA. 2016 Co-occurrence of mylodontid sloths and insights on their
418 potential distributions during the late Pleistocene. *Quat. Res.* **85**, 66–74.
419 (doi:10.1016/j.yqres.2015.11.009)
420 4. Borrero LA, Martin FM. 2012 Taphonomic observations on ground sloth bone and dung
421 from Cueva del Milodón, Ultima Esperanza, Chile: 100 years of research history. *Quat. Int.* **278**,
422 3–11. (doi:10.1016/j.quaint.2012.04.036)
423 5. Höss M, Dilling A, Currant A, Pääbo S. 1996 Molecular phylogeny of the extinct ground
424 sloth Mylodon darwinii. *Proc. Natl. Acad. Sci.* **93**, 181–185.
425 6. Greenwood AD, Castresana J, Feldmaier-Fuchs G, Pääbo S. 2001 A molecular
426 phylogeny of two extinct sloths. *Mol. Phylogenet. Evol.* **18**, 94–103.
427 (doi:10.1006/mpev.2000.0860)
428 7. Clack AA, MacPhee RDE, Poinar HN. 2012 Mylodon darwinii DNA sequences from
429 ancient fecal hair shafts. *Ann. Anat. - Anat. Anz.* **194**, 26–30. (doi:10.1016/j.aanat.2011.05.001)
430 8. Paijmans JLA, Gilbert MTP, Hofreiter M. 2013 Mitogenomic analyses from ancient
431 DNA. *Mol. Phylogenet. Evol.* **69**, 404–416. (doi:10.1016/j.ympev.2012.06.002)
432 9. Enk J *et al.* 2011 Complete Columbian mammoth mitogenome suggests interbreeding
433 with woolly mammoths. *Genome Biol.* **12**, R51. (doi:10.1186/gb-2011-12-5-r51)
434 10. Marsolier-Kergoat M-C, Palacio P, Berthonaud V, Maksud F, Stafford T, Bégouën R,
435 Elalouf J-M. 2015 Hunting the extinct steppe bison (Bison priscus) mitochondrial genome in the
436 Trois-Frères paleolithic painted cave. *PLOS ONE* **10**, e0128267.

437 (doi:10.1371/journal.pone.0128267)
438 11. Kistler L *et al.* 2015 Comparative and population mitogenomic analyses of Madagascar's
439 extinct, giant 'subfossil' lemurs. *J. Hum. Evol.* **79**, 45–54. (doi:10.1016/j.jhevol.2014.06.016)
440 12. Der Sarkissian C *et al.* 2015 Mitochondrial genomes reveal the extinct Hippidion as an
441 outgroup to all living equids. *Biol. Lett.* **11**, 20141058–20141058. (doi:10.1098/rsbl.2014.1058)
442 13. Heintzman PD, Zazula GD, Cahill JA, Reyes AV, MacPhee RDE, Shapiro B. 2015
443 Genomic data from extinct North American Camelops revise camel evolutionary history. *Mol.*
444 *Biol. Evol.* **32**, 2433–2440. (doi:10.1093/molbev/msv128)
445 14. Bon C, Berthonaud V, Maksud F, Labadie K, Poulain J, Artiguenave F, Wincker P, Aury
446 J-M, Elalouf J-M. 2012 Coprolites as a source of information on the genome and diet of the cave
447 hyena. *Proc. R. Soc. B Biol. Sci.* **279**, 2825–2830. (doi:10.1098/rspb.2012.0358)
448 15. Slater GJ, Cui P, Forasiepi AM, Lenz D, Tsangaras K, Voirin B, de Moraes-Barros N,
449 MacPhee RDE, Greenwood AD. 2016 Evolutionary relationships among extinct and extant
450 sloths: The evidence of mitogenomes and retroviruses. *Genome Biol. Evol.* **8**, 607–621.
451 (doi:10.1093/gbe/evw023)
452 16. Beaumont W, Beverly R, Southon J, Taylor RE. 2010 Bone preparation at the KCCAMS
453 laboratory. *Nucl. Instrum. Methods Phys. Res. Sect. B Beam Interact. Mater. At.* **268**, 906–909.
454 (doi:10.1016/j.nimb.2009.10.061)
455 17. Meyer M, Kircher M. 2010 Illumina sequencing library preparation for highly
456 multiplexed target capture and sequencing. *Cold Spring Harb. Protoc.* **2010**, pdb.prot5448.
457 (doi:10.1101/pdb.prot5448)
458 18. Delsuc F, Scally M, Madsen O, Stanhope MJ, de Jong WW, Catzeflis FM, Springer MS,
459 Douzery EJP. 2002 Molecular phylogeny of living xenarthrans and the impact of character and

460 taxon sampling on the placental tree rooting. *Mol. Biol. Evol.* **19**, 1656–1671.
461 19. Meredith RW *et al.* 2011 Impacts of the Cretaceous Terrestrial Revolution and KPg
462 extinction on mammal diversification. *Science* **334**, 521–524. (doi:10.1126/science.1211028)
463 20. Delsuc F, Superina M, Tilak M-K, Douzery EJP, Hassanin A. 2012 Molecular
464 phylogenetics unveils the ancient evolutionary origins of the enigmatic fairy armadillos. *Mol.*
465 *Phylogenet. Evol.* **62**, 673–680. (doi:10.1016/j.ympev.2011.11.008)
466 21. Gibb GC, Condamine FL, Kuch M, Enk J, Moraes-Barros N, Superina M, Poinar HN,
467 Delsuc F. 2016 Shotgun Mitogenomics Provides a Reference Phylogenetic Framework and
468 Timescale for Living Xenarthrans. *Mol. Biol. Evol.* **33**, 621–642. (doi:10.1093/molbev/msv250)
469 22. Enk JM, Devault AM, Kuch M, Murgha YE, Rouillard J-M, Poinar HN. 2014 Ancient
470 whole genome enrichment using baits built from modern DNA. *Mol. Biol. Evol.* **31**, 1292–1294.
471 (doi:10.1093/molbev/msu074)
472 23. Martin M. 2011 Cutadapt removes adapter sequences from high-throughput sequencing
473 reads. *EMBnet.journal* **17**, 10–12. (doi:10.14806/ej.17.1.200)
474 24. Simpson JT, Wong K, Jackman SD, Schein JE, Jones SJM, Birol I. 2009 ABySS: a
475 parallel assembler for short read sequence data. *Genome Res.* **19**, 1117–1123.
476 (doi:10.1101/gr.089532.108)
477 25. Kearse M *et al.* 2012 Geneious Basic: An integrated and extendable desktop software
478 platform for the organization and analysis of sequence data. *Bioinformatics* **28**, 1647–1649.
479 (doi:10.1093/bioinformatics/bts199)
480 26. Renaud G, Stenzel U, Kelso J. 2014 leeHom: adaptor trimming and merging for Illumina
481 sequencing reads. *Nucleic Acids Res.* **42**, e141. (doi:10.1093/nar/gku699)
482 27. Li H, Durbin R. 2009 Fast and accurate short read alignment with Burrows-Wheeler

483 transform. *Bioinforma. Oxf. Engl.* **25**, 1754–1760. (doi:10.1093/bioinformatics/btp324)
484 28. Stenzel U. 2017 network-aware-bwa. See https://github.com/mpieva/network-aware-bwa
485 (accessed on 9 May 2017).
486 29. Renaud G. 2015 libbam. See https://github.com/grenaud/libbam (accessed on 9 May
487 2017).
488 30. Stenzel U. 2017 biohazard. See https://bitbucket.org/ustenzel/biohazard (accessed on 9
489 May 2017).
490 31. Li H *et al.* 2009 The Sequence Alignment/Map format and SAMtools. *Bioinforma. Oxf.*
491 *Engl.* **25**, 2078–2079. (doi:10.1093/bioinformatics/btp352)
492 32. Jónsson H, Ginolhac A, Schubert M, Johnson PLF, Orlando L. 2013 mapDamage2.0: fast
493 approximate Bayesian estimates of ancient DNA damage parameters. *Bioinformatics* **29**, 1682–
494 1684. (doi:10.1093/bioinformatics/btt193)
495 33. Delsuc F *et al.* 2016 The phylogenetic affinities of the extinct glyptodonts. *Curr. Biol.* **26**,
496 R155–R156.
497 34. Li D, Luo R, Liu C-M, Leung C-M, Ting H-F, Sadakane K, Yamashita H, Lam T-W.
498 2016 MEGAHIT v1.0: A fast and scalable metagenome assembler driven by advanced
499 methodologies and community practices. *Methods San Diego Calif* **102**, 3–11.
500 (doi:10.1016/j.ymeth.2016.02.020)
501 35. Huson DH, Mitra S, Ruscheweyh H-J, Weber N, Schuster SC. 2011 Integrative analysis
502 of environmental sequences using MEGAN4. *Genome Res.* **21**, 1552–1560.
503 (doi:10.1101/gr.120618.111)
504 36. Ondov BD, Bergman NH, Phillippy AM. 2011 Interactive metagenomic visualization in a
505 Web browser. *BMC Bioinformatics* **12**, 385. (doi:10.1186/1471-2105-12-385)

506 37. Katoh K, Kuma K, Toh H, Miyata T. 2005 MAFFT version 5: improvement in accuracy
507 of multiple sequence alignment. *Nucleic Acids Res.* **33**, 511–518. (doi:10.1093/nar/gki198)
508 38. Castresana J. 2000 Selection of conserved blocks from multiple alignments for their use
509 in phylogenetic analysis. *Mol. Biol. Evol.* **17**, 540–552.
510 39. Lanfear R, Calcott B, Ho SYW, Guindon S. 2012 PartitionFinder: Combined selection of
511 partitioning schemes and substitution models for phylogenetic analyses. *Mol. Biol. Evol.* **29**,
512 1695–1701. (doi:10.1093/molbev/mss020)
513 40. Stamatakis A. 2014 RAxML version 8: a tool for phylogenetic analysis and post-analysis
514 of large phylogenies. *Bioinforma. Oxf. Engl.* **30**, 1312–1313.
515 (doi:10.1093/bioinformatics/btu033)
516 41. Ronquist F *et al.* 2012 MrBayes 3.2: Efficient Bayesian phylogenetic inference and
517 model choice across a large model space. *Syst. Biol.* **61**, 539–542. (doi:10.1093/sysbio/sys029)
518 42. Lartillot N, Rodrigue N, Stubbs D, Richer J. 2013 PhyloBayes MPI: phylogenetic
519 reconstruction with infinite mixtures of profiles in a parallel environment. *Syst. Biol.* **62**, 611–
520 615. (doi:10.1093/sysbio/syt022)
521 43. Lartillot N, Lepage T, Blanquart S. 2009 PhyloBayes 3: a Bayesian software package for
522 phylogenetic reconstruction and molecular dating. *Bioinforma. Oxf. Engl.* **25**, 2286–2288.
523 (doi:10.1093/bioinformatics/btp368)
524 44. Der Sarkissian C, Ermini L, Jónsson H, Alekseev AN, Crubezy E, Shapiro B, Orlando L.
525 2014 Shotgun microbial profiling of fossil remains. *Mol. Ecol.* **23**, 1780–1798.
526 (doi:10.1111/mec.12690)
527 45. Pääbo S *et al.* 2004 Genetic Analyses from Ancient DNA. *Annu. Rev. Genet.* **38**, 645–
528 679. (doi:10.1146/annurev.genet.37.110801.143214)

529 46. Toews DPL, Brelsford A. 2012 The biogeography of mitochondrial and nuclear
530 discordance in animals. *Mol. Ecol.* **21**, 3907–3930. (doi:10.1111/j.1365-294X.2012.05664.x)
531 47. Webb SD. 1985 The interrelationships of tree sloths and ground sloths. In *The evolution*
532 *and ecology of armadillos, sloths, and vermilinguas*, pp. 105–112.
533 48. Gaudin TJ. 2004 Phylogenetic relationships among sloths (Mammalia, Xenarthra,
534 Tardigrada): the craniodental evidence. *Zool. J. Linn. Soc.* **140**, 255–305.
535 49. Nyakatura JA. 2012 The convergent evolution of suspensory posture and locomotion in
536 tree sloths. *J. Mamm. Evol.* **19**, 225–234. (doi:10.1007/s10914-011-9174-x)
537 50. Pujos F, De Iuliis G, Cartelle C. 2017 A paleogeographic overview of tropical fossil
538 sloths: Towards an understanding of the origin of extant suspensory sloths? *J. Mamm. Evol.* **24**,
539 19–38. (doi:10.1007/s10914-016-9330-4)
540 51. Delsuc F, Vizcaíno SF, Douzery EJ. 2004 Influence of Tertiary paleoenvironmental
541 changes on the diversification of South American mammals: a relaxed molecular clock study
542 within xenarthrans. *BMC Evol. Biol.* **4**, 11.
543 52. Billet G, Hautier L, Muizon C de, Valentin X. 2011 Oldest cingulate skulls provide
544 congruence between morphological and molecular scenarios of armadillo evolution. *Proc. R.*
545 *Soc. Lond. B Biol. Sci.* **278**, 2791–2797. (doi:10.1098/rspb.2010.2443)
546 53. Heath TA, Huelsenbeck JP, Stadler T. 2014 The fossilized birth–death process for
547 coherent calibration of divergence-time estimates. *Proc. Natl. Acad. Sci.* **111**, E2957–E2966.
548 (doi:10.1073/pnas.1319091111)
549 54. Marshall LG, Sempere T. 1993 Evolution of the Neotropical Cenozoic land mammal
550 fauna in its geochronologic, stratigraphic, and tectonic context. In *Biological relationships*
551 *between Africa and South America*, pp. 329–392.

552 55. Patterson B, Pascual R. 1968 The Fossil Mammal Fauna of South America. *Q. Rev. Biol.*
553 **43**, 409–451. (doi:10.1086/405916)
554 56. Martin PS, Klein RG. 1989 *Quaternary Extinctions: A Prehistoric Revolution*. University
555 of Arizona Press.
556 57. Fariña RA, Vizcaíno SF, Iuliis GD. 2013 *Megafauna: Giant Beasts of Pleistocene South*
557 *America*. Indiana University Press.
558
559

Figure legends

Figure 1. (*a*) DNA damage profiles from the *Mylodon* bone sample (12,880 ± 35 ^{14}C yrpb) compared to a fossil glyptodont sample (*Doedicurus* sp.) dated at (12,015 ± 50 ^{14}C yrpb), a 40-year-old museum specimen of greater fairy armadillo (*Calyptophractus retusus*), and three modern xenarthran samples. (*b*) Taxonomic assignation of 223 contigs assembled from *Mylodon* shotgun reads represented with Krona.

Figure 2. Bayesian consensus phylograms of Pilosa obtained under the site-heterogeneous CAT-GTR+G_4 mixture model for the mitogenomic (*a*) and nuclear (*b*) datasets. Values at nodes represent clade posterior probabilities under the CAT model (PP_{CAT}), mixed model (PP_{PART}), and maximum likelihood bootstrap percentages under a partitioned model (BP_{ML}). Asterisks indicate maximum support from all statistical indices. The complete phylograms are available in the electronic supplementary material (electronic supplementary material, figures S3-S8). Graphical representation and taxon images derive from Gibb et al. [21].

Figure 3. Bayesian chronograms of Pilosa obtained using a rate-autocorrelated log-normal relaxed molecular clock model under the CAT-GTR+G_4 mixture model with a birth death prior on the diversification process, and six soft calibration constraints for the mitogenomic (*a*) and nuclear (*b*) datasets. Mean divergence dates and associated 95% credibility intervals are represented as node bars. Plain black node bars indicated calibration constraints. The main geological periods follow Geological Time Scale of the Geological Society of America (E = Early, M = Middle, L = Late; Paleo. = Paleocene, Pli. = Pliocene, P. = Pleistocene). The complete chronograms are available in the electronic supplementary material (electronic

583 supplementary material, figures S9, S10). Graphical representation and taxon images derive from
584 Gibb et al. [21].
585

586 # Tables

587

588 **Table 1.** Divergence time estimates for the main xenarthran nodes inferred using the site-heterogeneous CAT-GTR+G_4
589 substitution model and an autocorrelated log-normal (LN) relaxed molecular clock model. Mean posterior estimates, associated
590 standard errors, and 95% credibility intervals are expressed in million years ago (Mean date ± SD [95% CredI]).

Nodes	Mitogenomes	Nuclear exons
XENARTHRA*	67.3 ± 3.2 [59.9 – 71.4]	69.3 ± 2.2 [63.5 – 71.8]
PILOSA MRCA* (anteaters + sloths)	55.6 ± 4.4 [46.4 – 63.2]	61.2 ± 2.5 [55.4 – 65.0]
Folivora MRCA* (sloths)	24.8 ± 6.2 [15.8 – 37.6]	27.7 ± 4.0 [19.6 – 35.9]
Mylodondidae + Megalonychidae (two-fingered sloths)	21.9 ± 5.7 [13.3 – 33.9]	22.5 ± 3.7 [15.5 – 30.6]
Megalonychidae MRCA (two-fingered sloths)	4.7 ± 1.5 [2.5 – 8.3]	3.8 ± 1.1 [2.2 – 6.5]
Bradypodidae MRCA (three-fingered sloths)	14.3 ± 4.1 [8.4 – 23.1]	12.1 ± 2.4 [7.8 – 17.5]
B. pygmaeus / others	5.4 ± 1.8 [2.8 – 9.6]	4.5 ± 1.1 [2.7 – 7.0]
B. tridactylus / *B. variegatus*	4.2 ± 1.5 [2.2 – 7.7]	3.9 ± 1.0 [2.3 – 6.2]
Vermilingua MRCA* (anteaters)	34.2 ± 5.1 [23.9 – 44.2]	43.7 ± 3.2 [36.6 – 49.7]
Myrmecophaga / Tamandua	10.7 ± 3.0 [5.6 – 17.6]	11.9 ± 2.1 [8.4 – 16.7]

T. mexicana / *T. tetradactyla*	0.8 ± 0.3 [0.4 – 1.5]	2.0 ± 0.5 [1.2 – 3.2]
CINGULATA MRCA (armadillos)	44.2 ± 3.5 [37.9 – 51.5]	42.3 ± 2.4 [37.7 – 47.2]
Dasypodidae MRCA (Long-nosed armadillos)	11.5 ± 3.4 [7.2 – 20.4]	8.7 ± 1.6 [6.3 – 12.4]
Chlamyphoridae MRCA	36.6 ± 3.3 [31.2 – 44.1]	33.4 ± 2.1 [29.7 – 38.2]
Euphractinae MRCA (Hairy armadillos)	10.3 ± 2.7 [6.4 – 16.6]	6.1 ± 1.3 [4.0 – 9.2]
Chlamyphorinae / Tolypeutinae	32.4 ± 3.1 [27.8 – 39.7]	31.5 ± 2.0 [28.0 – 36.0]
Chlamyphorinae MRCA (Fairy armadillos)	19.7 ± 2.7 [15.5 – 26.3]	14.8 ± 2.4 [10.4 – 19.9]
Tolypeutinae MRCA*	25.8 ± 2.6 [22.5 – 32.5]	23.7 ± 1.3 [21.7 – 27.1]
Tolypeutes / *Cabassous*	22.5 ± 2.5 [19.1 – 28.8]	21.1 ± 1.5 [18.6 – 24.6]
Tolypeutes MRCA	13.7 ± 2.0 [10.7 – 18.4]	11.9 ± 1.5 [9.2 – 15.2]
Cabassous chacoensis / *C. unicinctus*	8.4 ± 1.5 [5.9 – 11.9]	6.5 ± 1.4 [4.1 – 9.4]

Notes -- SD: Standard Deviation; 95% CredI: 95% Credibility Interval; *: Used as a priori calibration constraints; MRCA: Most Recent Common Ancestor.

(a)

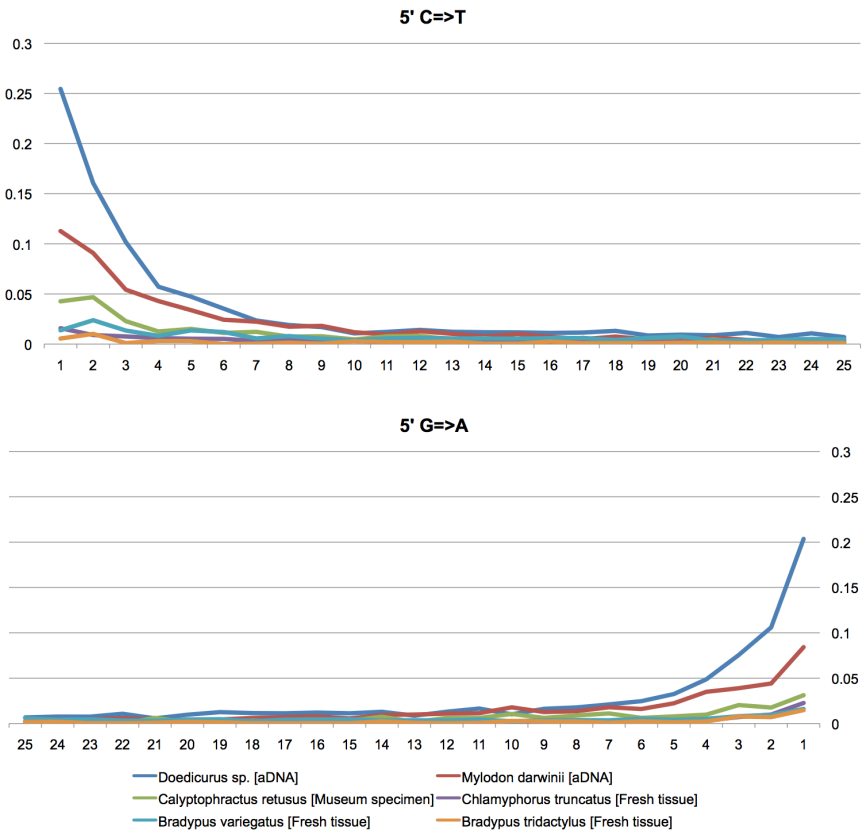
5' C=>T
0.3
0.25
0.2
0.15
0.1
0.05
0
1 2 3 4 5 6 7 8 9 10 11 12 13 14 15 16 17 18 19 20 21 22 23 24 25
5' G=>A
25 24 23 22 21 20 19 18 17 16 15 14 13 12 11 10 9 8 7 6 5 4 3 2 1
Doedicurus sp. [aDNA]
Mylodon darwinii [aDNA]
Calyptophractus retusus [Museum specimen]
Chlamyphorus truncatus [Fresh tissue]
Bradypus variegatus [Fresh tissue]
Bradypus tridactylus [Fresh tissue]

(b)

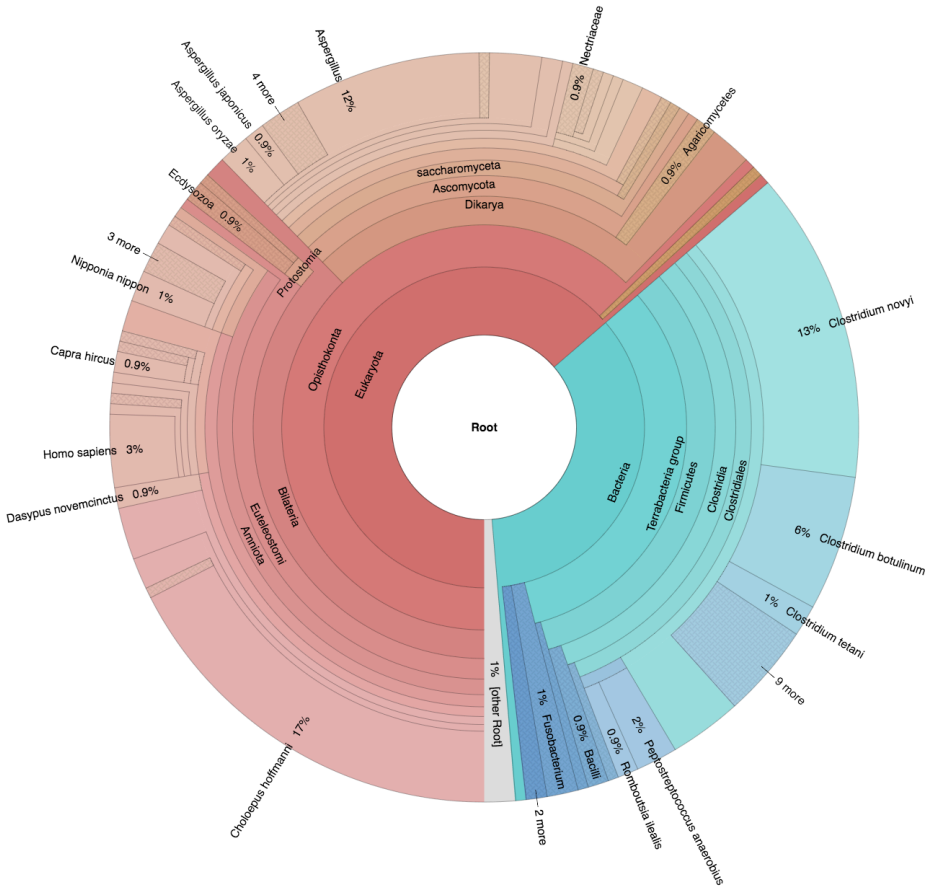
Root
Eukaryota
Opisthokonta
Metazoa
Bilateria
Eutelostomi
Ammiota
Chordata
Homo sapiens 3%
Dasypus novemcinctus 0.9%
Capra hircus 0.9%
Nipponia nippon 1%
3 more
Ecdysozoa 0.9%
Protostomia
Arthropoda
Cholaepus hoffmanni 17%
Dikarya
Ascomycota
saccharomyceta
Aspergillus oryzae 1%
Aspergillus japonicus 0.9%
4 more
Aspergillus 12%
Nectriaceae 0.9%
Agaricomycetes 0.9%
Bacteria
Terrabacteria group
Firmicutes
Clostridia
Clostridiales
13% Clostridium novyi
6% Clostridium botulinum
1% Clostridium tetani
9 more
1% [other Root]
2 more
1% Fusobacterium
0.9% Bacilli
0.9% Romboutsia ilealis
2% Peptostreptococcus anaerobius

(a) mitogenomes

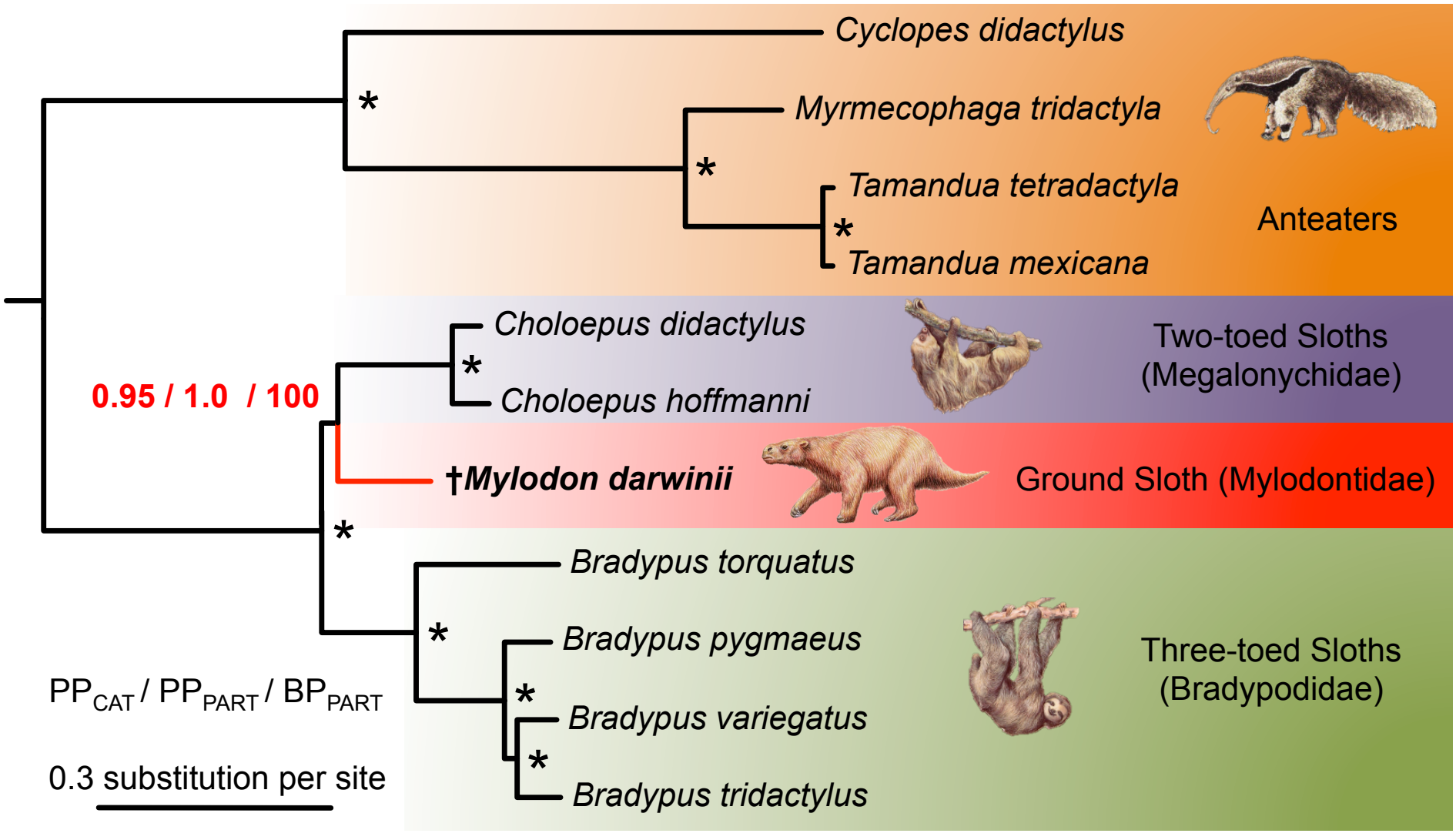

(b) nuclear exons